J. Protozool., 35(4), 1988, pp. 607–617

Duboscquella cachoni N. Sp., a Parasitic Dinoflagellate Lethal to Its Tintinnine Host *Eutintinnus pectinis*[1]

D. WAYNE COATS

Chesapeake Bay Institute, The Johns Hopkins University, 4800 Atwell Road, Shady Side, Maryland 20764

ABSTRACT. The parasitic dinoflagellate *Duboscquella cachoni* n. sp. is described from infestations of the tintinnine ciliate *Eutintinnus pectinis* collected from the Chesapeake Bay, a major North American estuary located on the east coast of the United States. Examination of parasite life history, morphology, and developmental processes reveals that *D. cachoni* differs from other members of the genus by the structure of the trophont, the pattern of sporogenesis, and spore morphology. Sporogenesis results in the production of either biflagellated macrospores, microspores with a single flagellum, or a cyst-like stage. The number of spores formed per infestation and their survival outside the host vary with spore type. Infested ciliates are apparently unable to reproduce, and infestations are always fatal to *E. pectinis*. Aspects of parasite biology and observations of a natural host–parasite assemblage suggest that *D. cachoni* may have a significant impact on its host's population dynamics.

EARLY reports on dinoflagellate infestations of tintinnine ciliates established the taxonomic affinity of the parasite and emphasized the morphology and development of the dinospore, a flagellated dispersal stage (7, 8, 12); however, sufficient morphological criteria to distinguish species were not furnished, and dinoflagellate infestations reported for a variety of tintinnine hosts were attributed to a single organism, *Duboscquella tintinnicola* (4). Grassé (reported by Chatton [5]) recognized morphological variations among spores resulting from different infestations and described a second species, *D. anisospora*, characterized by dinospores of unequal size and a trophont that had a curiously ribbed surface. Most recently, Cachon (2) examined the life cycle and cytology of several *Duboscquella* spp. and stressed differences in trophont morphology as criteria for differentiating species. He expanded the genus to include five new species and reported infestations from a variety of planktonic protists including non-tintinnine ciliates and dinoflagellates (for review see [3]).

Duboscquella infestations of tintinnine ciliates are passively transmitted when dinospores are ingested by susceptible hosts (2). Once inside the host, spores lose their flagella, differentiate into trophonts, and enter an extended growth phase. The episome (=epicone) of the trophont is covered by a thickened cuticle, the shield, which is limited peripherally by a fibrous ring, the perinema. Smaller fibers emanate from the perinema and extend beneath the shield. These fibers are organized in species-specific patterns and are usually associated with furrows or grooves in the shield. The lamina pharyngea, a funnel-shaped skeletal structure of uncertain function, is attached to the perinema and marks the ventral surface of the parasite. In several *Duboscquella* species, final growth of the trophont involves an elaborate morphogenetic process that results in the phagocytosis of a substantial portion of the host cytoplasm; however, other species consume the host without forming a food vacuole. In either case, the trophont phase is followed by palintomic sporogenesis (i.e. successive nuclear and cytoplasmic divisions without interruption = palintomy) which produces numerous biflagellate spores. Both macrospores and microspores may be formed by the same species, but only one type is released from a given host.

Tintinnine ciliates collected from Chesapeake Bay in the early to mid-1980's commonly harbored endoparasites that resembled dinoflagellates of the genus *Duboscquella*. Parasites were especially prevalent in *Eutintinnus pectinis*, a dominant tintinnine species during summer that frequently reached densities in excess of 10^3 cells liter^{-1}. Observations on the cytology and life history of these parasites indicated that *E. pectinis* was infested by a previously unreported species of dinoflagellate. The current description of *Duboscquella cachoni* n. sp. emphasizes aspects of trophont morphology and provides details of other life history stages. Estimates of parasite development time, spore production, and spore survival are also furnished.

MATERIALS AND METHODS

Eutintinnus pectinis parasitized by *Duboscquella cachoni* were collected from Chesapeake Bay during the summer, May–September, of 1980 to 1987. Samples obtained on cruises aboard the R/V Ridgley Warfield were taken at routine stations positioned along the central axis of the Bay (Fig. 1). Unconcentrated

[1] Research was supported by National Science Foundation Grant OCE-8515834. Contribution No. 283 of the Chesapeake Bay Institute, The Johns Hopkins University. I wish to express my gratitude to J. Heisler for technical assistance, L. Reid for illustrations, and C. Dolan for translating pertinent sections of referenced French manuscripts to English. I also thank T. K. Maugel and the Laboratory for Ultrastructural Research, Department of Zoology, University of Maryland, College Park, for use of their facilities; and the Captain and crew of the R/V Ridgely Warfield for ship operations and on-deck assistance.

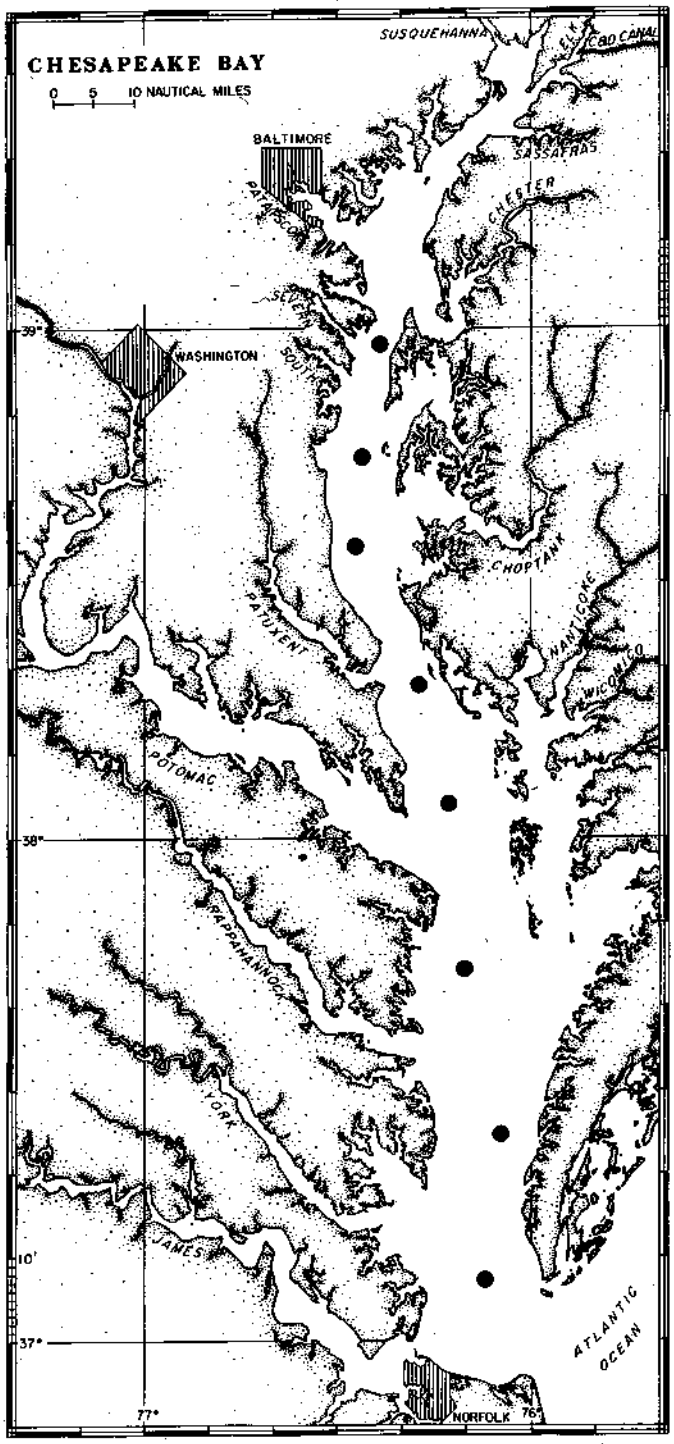

Fig. 1. Routine stations for research cruises on Chesapeake Bay from 1980 to 1987 (●).

samples and material collected on 20-μm Nitex screening were fixed in a modified Bouin's solution (6). Specimens stained with acidulated alum hematoxylin (9), Masson's modified trichome (11), or protargol silver impregnation (11) were viewed and photographed on a Zeiss WL brightfield/phase microscope equipped with an Olympus OM-2N camera. Cellular measurements are for protargol-impregnated specimens and were made using a filar micrometer; means are reported with standard errors (±SE) and sample sizes (n).

Observations of living parasites were made aboard ship using freshly collected samples. Infected ciliates were washed by micropipetting cells through several changes of 0.45-μm filtered Bay water and individually transferred to wet-mount slide preparations. Wet mounts consisted of ~0.1 ml filtered water sealed beneath a coverslip and enclosed within a vaspar ring (50% petroleum jelly : 50% paraffin) of sufficient thickness to provided an ample air space. Isolated specimens were placed in humidity chambers, held in a Percival incubator at ambient Bay temperature (23–27°C), and periodically examined and photographed. These direct observations provided data on developmental events, the duration of sporogenesis (i.e. the interval between ingestion of the host cell and release of spores), the number of spores produced infestation^{-1}, and survival time of spores.

Information on the population dynamics of *D. cachoni* was obtained through the study of a natural host–parasite assemblage. A 200-liter Nalgene tank was filled with Bay water containing parasitized *Eutintinnus pectinis* and incubated on deck as previously described (6). The isolated population was exposed to the natural light regime, maintained at ambient temperature (~24°C), and thoroughly mixed and sampled at 4–6-h intervals over 36 h with a final sample taken at 48 h. The relative frequencies of non-parasitized hosts and cells infested by *D. cachoni* were determined from hematoxylin preparations with ≥100 specimens examined per sample. The occurrence of sporogenic stages and host population density were determined by inverted microscopy (15) at ×200 with four 50-ml aliquots of Bouin's-preserved unconcentrated sample analyzed for each sampling period. Data for trophont abundance were obtained by multiplying host density and percent infested hosts.

For scanning electron microscopy (SEM), specimens were micropipetted to a Swinnex filter unit (Millipore Corp., Bedford, MA) equipped with a 0.6-μm Nucleopore filter and flooded with a Karnovsky's-sea water fixative (0.2 M cacodylate buffer, 10% paraformaldehyde, 25% glutaraldehyde, and 75% sea water in a 5:2:1:2 ratio). Cells were preserved in this solution for ≥2 h and then drawn onto the filter. The filter was removed from the filter unit, washed in several changes of distilled water, placed in Parducz's fixative (13) for 30 min, again washed in distilled water, dehydrated in a graded ethanol series, dried using a Denton DCP-1 critical point apparatus, coated with a gold–palladium alloy, and examined on an AMR 1000A scanning electron microscope.

Pearson correlation coefficients and significant probabilities (P) were calculated for nuclear size and dimension of the perinematic ring relative to trophont body size and for nucleolar diameter vs. maximum nuclear dimension.

RESULTS

Duboscquella cachoni n. sp. (Figs. 2–17; 19–34)

Diagnosis. Trophonts spherical to ovoid, 3.4–47.1 × 3.4–12.8 μm; perinema forms a closed elliptical ring measuring 5.0–33.9 μm along the major axis; lamina pharyngea broadly funnel-shaped, ~2 μm in maximum diameter; shield convex, often inconspicuous, and creased by a short sagittal furrow; nucleus spherical to ovoid, 2.2–15.7 μm in maximum dimension; eccentric nucleolus of immature trophonts either fragmented or absent in mature trophonts; chromosomes not condensed during trophont growth. Post-phagotrophic stage cylindrical, 33.7–95.0 × 12.1–20.2 μm (70.8 ± 2.66 × 14.5 ± 0.29 μm). Macrospores bipartite, 5.4–7.9 × 3.9–4.9 μm (6.6 ± 0.10 × 4.4 ± 0.05 μm); transverse flagellum ~10 μm long; posterior flagellum ~15 μm long; nucleus ovoid, ~2 × 3 μm. Microspores spherical, 1.6–3.1 μm (2.2 ± 0.08 μm) in diameter; single flagellum ~5 μm long; nucleus ovoid, ~1 × 2 μm. Cyst-like spores spindle-shaped, 4.3–7.6 × 1.0–1.8 μm (6.0 ± 0.20 × 1.4 ± 0.05 μm).

Type host. The tintinnine ciliate *Eutintinnus pectinis.*

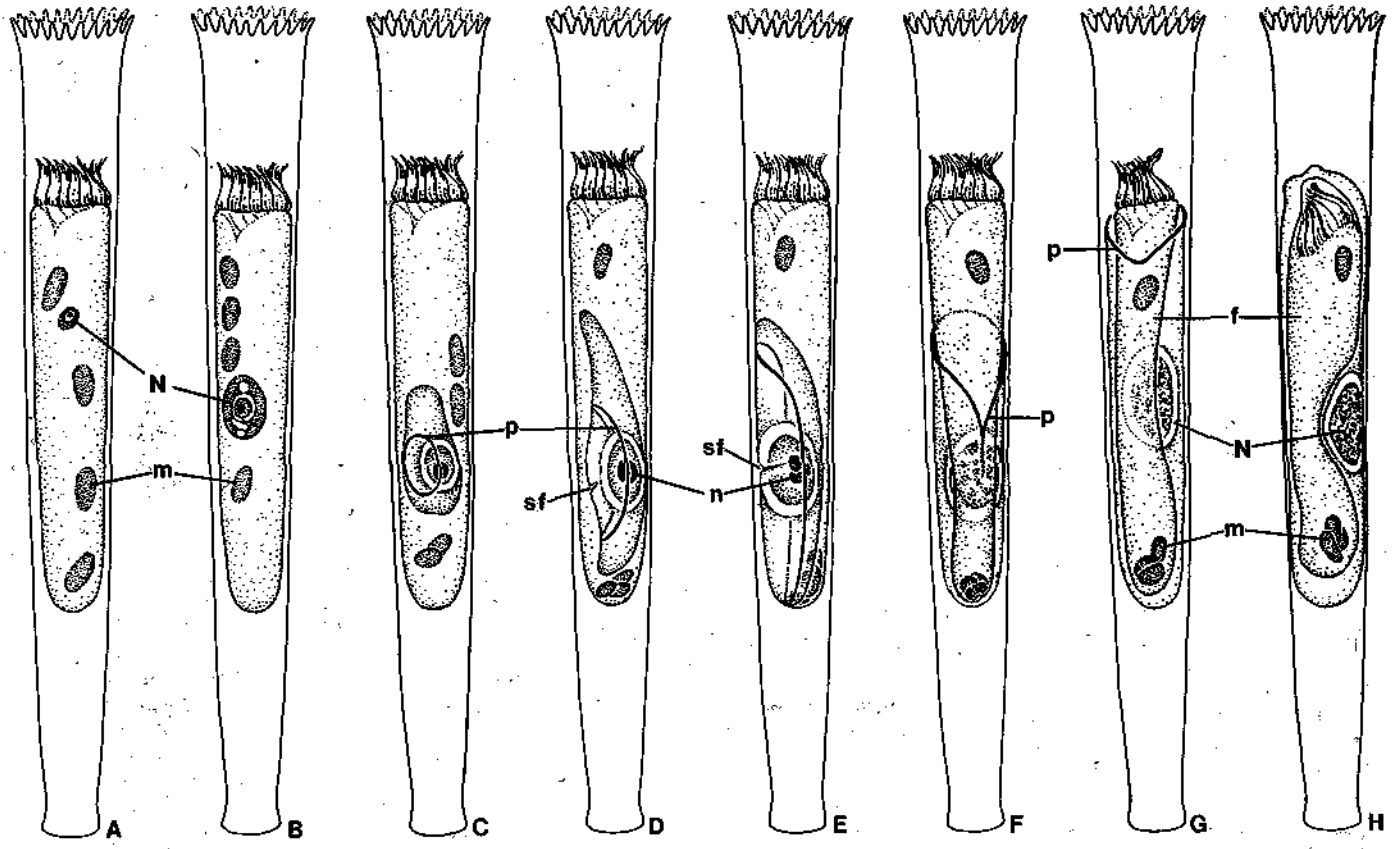

Fig. 2. Semi-diagrammatic illustrations of *Eutintinnus pectinis* parasitized by *Duboscquella cachoni*. The parasite is shown in developmental stages from early infestation (A), through growth of the trophont (B–E), and the phagotrophic phase (F–H); food mass (f), ciliate macronuclei (m), parasite nucleus (N), nucleolus (n), perinema (p), sagittal furrow (sf).

Type locality. Surface waters of the Chesapeake Bay, a moderately stratified estuary bordered by the states of Maryland and Virginia, USA.

Type material. Syntypes, slides with protargol-impregnated *E. pectinis* infested by trophonts of *D. cachoni*, have been deposited at the National Protozoan Type Collection, National Museum of Natural History, Washington, D.C., and given the following registration numbers: 40528 and 40529.

Etymology. The species is named in honor of Professor Jean Cachon, whose work has contributed significantly to our knowledge of the genus *Duboscquella* and many other parasitic dinoflagellates.

Morphology and development of the trophont. The smallest trophonts of *D. cachoni* measure ~3 μm in diameter, lack flagella, and are usually located in the anterior third of the host cytoplasm (Table I; Figs. 2A, 3). Slightly later stages in trophont development are ovoid in profile, contain large vacuoles, and are often positioned more posteriorly in the host (Figs. 2B, 4). With continued growth, the trophont elongates, and pseudopod-like extensions are directed anteriorly in the host cytoplasm (Fig. 5). More mature trophonts have a granular cytoplasm, occupy much of the host cell, and measure <50 μm in length with a width nearly equal to that of the ciliate (Figs. 2D, E, 6, 7). In living specimens, the boundary between host and parasite cytoplasm is not well defined, and trophonts appear as opaque yellowish masses that are refractile in phase contrast microscopy (Fig. 8).

Early trophonts have a spherical nucleus (~2 μm diam.) with a relatively large (~1.5 μm) eccentric nucleolus (Figs. 2A, 3). A substantial increase in nuclear dimension occurs during growth of the trophont, and nuclear measurements are strongly correlated ($P \ll 0.01$) with parasite length (Fig. 18A). Mature trophonts (i.e. cells nearing the phagotrophic stage) have a voluminous ovoid nucleus (8–10 × ≤16 μm) that is located in the center of the parasite (Figs. 7, 16). The nucleolus also enlarges during cell growth and is closely correlated in size ($P \ll 0.01$) with maximum nuclear dimension (Fig. 18B). The chromosomes of trophont nuclei are not conspicuous in stained specimens and the nucleoplasm of early to mid-trophonts forms a relatively homogeneous mass that is withdrawn from the nuclear envelope (Figs. 4–6, 14). Numerous argentophilic granules are evenly distributed over the surface of the nucleus and appear intimately associated with the nuclear envelope (Fig. 14). The nucleoplasm of mature trophonts is condensed into irregular clumps, and the nucleolus is either fragmented into small globules or absent (Figs. 7, 16).

The perinema is absent in early trophonts and first appears as a small ring (~5 μm diam.) on the surface of individuals that measure 10–15 μm in length (Fig. 2C). This structure, which encircles the episome, becomes elliptical during trophont maturation, and measurements for the major axis of the perinematic ring are closely correlated ($P \ll 0.01$) with parasite length (Fig. 18C). The episome of large trophonts is greatly expanded and the perinema curves around the surface of the parasite to form the outline of a saddle (Figs. 2D, E, 10). The perinema of well stained specimens appears as a complete loop that is not broken in the vicinity of the lamina pharyngea (Fig. 12).

The shield of *D. cachoni* is not obvious in early to mid-trophonts even when the perinema is well developed; however, the shield of more mature trophonts is distinct and conveys a highly convex profile to the episome (Fig. 13). At this stage, a thin transparent space is located between the shield and the pellicle of the host. The sagittal furrow is directed along the minor axis of the perinematic ring and forms a narrow groove

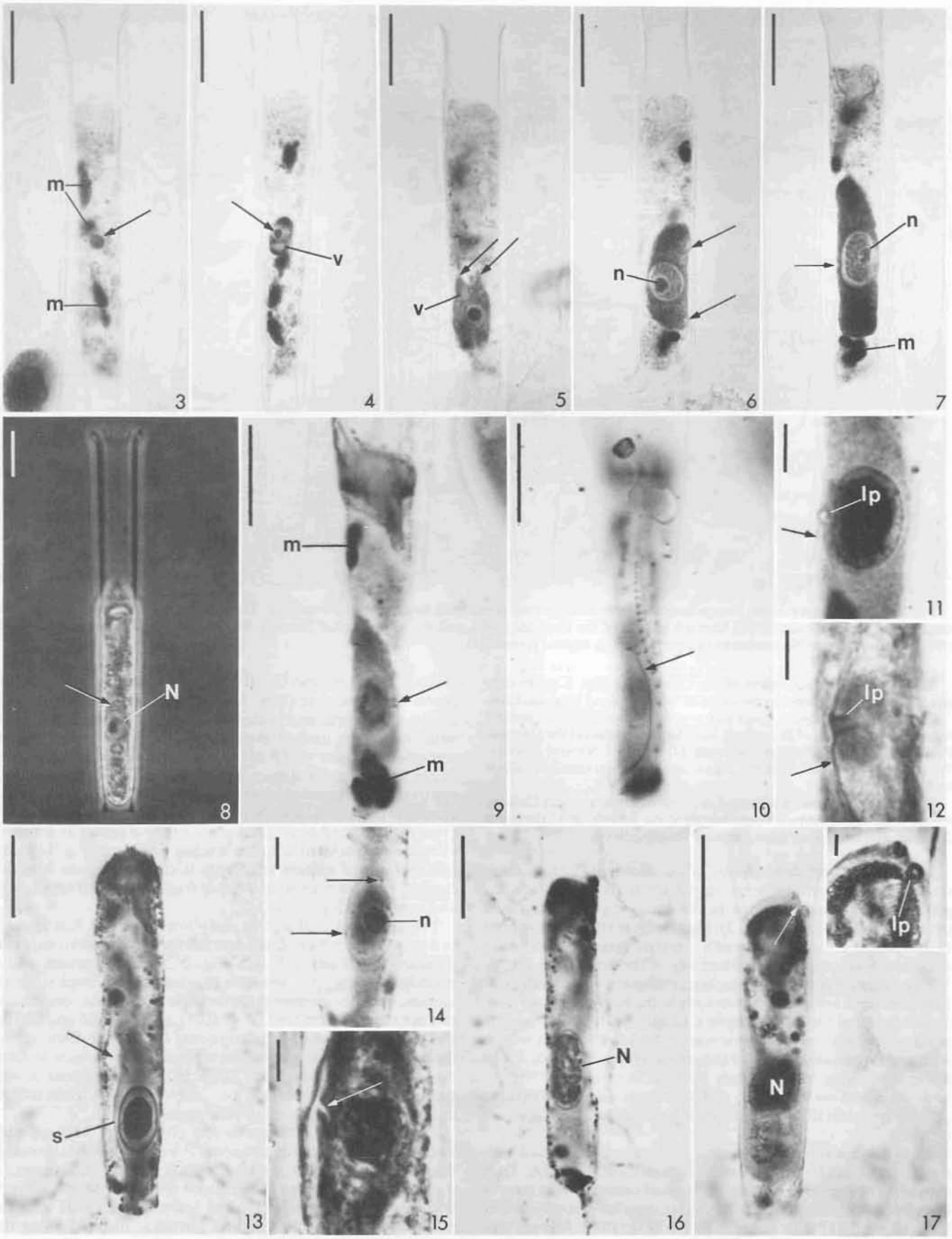
m
m
3
v
4
v
5
n
6
n
m
7
N
8
m
m
9
10
lp
11
lp
12
s
13
n
14
15
N
16
N
lp
17

~1 μm wide and 2–3 μm deep that arches over the central quarter of the shield (Figs. 2D, 15). One or more smaller grooves are occasionally evident, but these are not organized in a regular pattern. Most specimens appear to lack fibrillar extensions of the perinema; however, very thin fibers are sometimes visible in densely stained, mature trophonts. When present, these fibers are directed radially beneath the shield, appear to extend for only a few micrometers, and are not accompanied by furrows. Late in trophont development, the episome is less convex; the shield is again inconspicuous, and the sagittal furrow is not prominent.

The lamina pharyngea, which develops after the episome starts to expand, is located just posterior to the perinema and near the minor axis of the perinematic ring (Figs. 9, 12). The lamina pharyngea is broadly funnel-shaped in longitudinal view, has a maximum dimension of 1.9 ± 0.08 μm (n = 10) near the perinema, and is directed beneath and toward the center of the shield. In ventral view, the lamina pharyngea forms a short sinistral helix that broadens as it extends dorsally into the cytoplasm (Fig. 11).

Phagocytosis. Phagocytosis by *D. cachoni* is rapid and typically results in the complete ingestion of the host. Early in this process, the parasite ruptures through the posterior end of the ciliate and the hyposome (=hypocone) invaginates to form a deep cavity. This cavity, the presumptive food vacuole, envelops the host from posterior to anterior and is defined at its leading edge by the perinema (Fig. 2F, G). During phagocytosis, the perinema forms a teardrop contour that is oriented diagonally over the surface of the host. The trailing end of this profile stains less densely with protargol and gives the impression that the perinema is being closed in a zipper-like fashion. The perinematic ring progressively decreases in size and near the end of ingestion is associated with a pucker on the outer surface of the parasite (Fig. 17). The lamina pharyngea remains attached to the perinema and is eventually positioned beneath this pucker (Fig. 17, inset). Following phagocytosis, the episome covers the outer surface of the parasite, the hyposomal membrane is completely internalized, and the perinematic ring and lamina pharyngea are resorbed.

At the end of ingestion, *D. cachoni* is a large cylindrical organism (14.5 ± 0.29 × 70.8 ± 2.66 μm; n = 32) that contains a massive food vacuole surrounded by a thin layer of cytoplasm (Figs. 2H, 19). The nucleus, which remains equatorial in position, is displaced laterally by the food vacuole and pressed against the cell periphery. Consequently, the shape of the nucleus is somewhat discoidal, but slightly curved in cross section. Digestion proceeds quickly and reduces the food vacuole to an opaque mass that is usually positioned near the posterior end of the parasite. Simultaneously, a transparent area develops around the opaque food mass and soon occupies much of the cell's interior.

Sporogenesis and spore morphology. Sporogenesis in *D. cachoni* occurs by palintomy and begins soon after the completion of phagocytosis. Sporogenic divisions proceed in rapid succession with fissions occurring at 15–20-min intervals. The first few cytoplasmic divisions are almost synchronous and divide the parasite transversely into sporocytes of approximately equal size (Fig. 20). The large transparent vacuole formed during digestion is divided at each cytokinesis; however, the condensed food mass typically remains intact and passes to the most posterior sporocyte (Figs. 20, 21). This cell divides more slowly than the other sporocytes, resulting in asynchronous cell division that usually proceeds along an anterior to posterior gradient. After several divisions, the plane of cytokinesis becomes oblique to longitudinal, and a tightly packed cluster of sporocytes soon forms (Figs. 22, 23). Early in the sporogenic process, cytokinesis does not immediately follow karyokinesis and large sporocytes often contain several nuclei (Fig. 25). Nuclear and cell division are more closely coupled later in sporogenesis and small sporocytes usually contain only one or two nuclei (Fig. 26). Chromosomes are condensed during divisions and five short v-shaped profiles are distributed to each daughter nucleus (Fig. 24). Sporocytes often remain clustered for an extended time following the last fission but eventually separate as sporogenesis culminates in the formation of either microspores, macrospores, or "cysts."

Microspores of *D. cachoni* (Figs. 27–29) are spherical, measure 2.2 ± 0.08 μm in diameter (n = 30), and possess a single short flagellum (~5 μm). An ovoid to spherical nucleus (1.3 ± 0.03 × 1.7 ± 0.06 μm) is the only prominent cytoplasmic inclusion. Microspores are weakly motile and disperse slowly from the host lorica. They usually exhibit a random jerky motion but occasionally have bursts of more directed movement.

Macrospores (Figs. 30–32) average 4.5 ± 0.05 × 6.6 ± 0.10 μm (n = 30) and have a shallow girdle that separates the cell into a globular episome and a smaller hyposome. The episome protrudes asymmetrically over the hyposome and produces a cell contour that is rounded on one surface and strongly indented on the opposite side. A spherical to ovoid nucleus is positioned near the girdle and measures 2.5 ± 0.04 × 2.9 ± 0.05 μm (n = 30). Two flagella of unequal length emerge from a pair of basal bodies located equatorially on the rounded surface of the cell. In living specimens, the shorter flagellum (~10 μm) wraps transversely around the cell at the level of the girdle and the

←

Figs. 3–17. Morphology and development of *D. cachoni* through the phagotrophic phase. Bars = 20 μm unless otherwise noted. **3–7.** Sequential stages in trophont development; hematoxylin preparations. **3.** *E. pectinis* infested by a very early trophont (arrow); host macronuclei (m). **4.** A young, ovoid trophont containing a large cytoplasmic vacuole (v) and spherical nucleus with a densely staining nucleolus (arrow). **5.** An intermediate stage in trophont growth that still contains vacuoles (v) and has pseudopod-like structures (arrows) extending into the host's cytoplasm. **6.** A large trophont prior to fragmentation of the nucleolus (n). Arrows indicate the margins of the episome. **7.** A mature trophont possessing an ovoid nucleus and fragmented nucleolus (n). Also evident are the sagittal furrow (arrow) and an aggregate of host macronuclei (m) at the posterior end of the ciliate. **8.** Phase contrast image of a living host infested by *D. cachoni.* Cellular limits of the parasite (arrow) are not well defined, but the size of its nucleus (N) indicates that this is an immature trophont. **9–17.** Protargol-impregnated specimens. **9.** A nearly mature trophont showing the position of the lamina pharyngea (arrow); host macronuclei (m). **10.** Same individual as Fig. 9 with a portion of the perinematic ring (arrow) in focus. **11.** Ventral view of the lamina pharyngea (lp) and perinematic ring (arrow). Bar = 5 μm. **12.** The lamina pharyngea (lp), shown in profile, is positioned immediately posterior to (i.e. beneath) the perinema (arrow). Bar = 5 μm. **13.** Trophont with a distinct clear zone (arrow) between the convex shield (s) and the host's pellicle. **14.** Same specimen as Fig. 13 showing the relatively homogeneous nature of the nucleoplasm, the dense nucleolus (n), and several argentophilic granules (arrows) associated with the nuclear envelope. Bar = 5 μm. **15.** Sagittal furrow (arrow) of an impregnated trophont viewed with phase contrast optics. Bar = 5 μm. **16.** Mature trophont that has a large ovoid nucleus (N), irregularly condensed nucleoplasm, and lacks a nucleolus. **17.** *D. cachoni* at the end of the phagotrophic phase. Arrow marks a pucker formed at the closure of the perinematic ring; parasite nucleus (N). Inset is an enlargement of the pucker and shows the lamina pharyngea (lp) in cross-section; phase contrast. Bar = 2.5 μm.

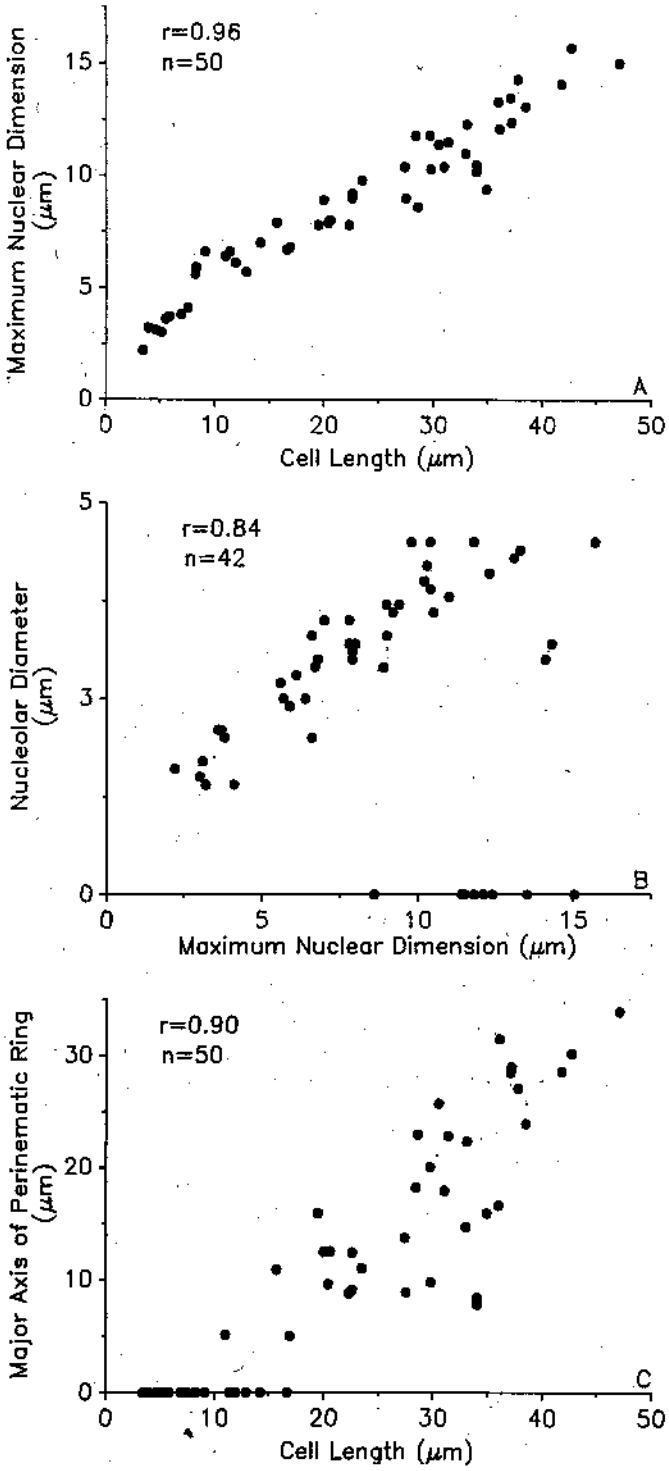

longer (~15 μm) extends posteriorly. Macrospores are highly motile, swim in short rapid bursts, and disperse rapidly from the host lorica.

A cyst-like spore was produced by some *D. cachoni* infestations. These spores were never motile but could be easily shaken from the lorica. After the last sporogenic division, "encysting" cells were tear-drop in shape (Fig. 33) but soon elongated into spindle-shaped "cysts" (Fig. 34). In protargol preparations, "cysts" measured 1.4 ± 0.05 × 6.0 ± 0.20 μm (n = 20) and phase contrast microscopy revealed a spherical to ovoid cytoplasmic inclusion (Fig. 34, inset) that was similar in size to the nucleus of microspores (Table I). Unfortunately, attempts to confirm the nuclear nature of this structure through cytological techniques were not successful as the stains employed did not penetrate the "cyst."

Observations on spore production, spore survival, and duration of sporogenesis. The incidence of microspore, macrospore, and "cyst" formation for *E. pectinis* infested by *D. cachoni* was 73.5, 20.4, and 6.1%, respectively (n = 49). The number of spores produced infestation^{-1} ranged from 240 to 897 (448 ± 39.9; n = 16) for microspores, 50 to 70 (57 ± 2.5; n = 6) for macrospores, and 589 to 720 (644 ± 32.1; n = 3) for "cysts." In wet mount preparations, macrospores remained active for a few hours, then lost their motility and lysed 4–6 h after leaving the host lorica. Microspores were only active for a short time (~1 h) but often persisted for 15–20 h before lysing. "Cysts" showed no signs of deteriorating with time and were still intact when preserved 5 days after their formation.

The duration of sporogenesis (i.e. the interval from ingestion of the host to release of spores), averaged 4.7 ± 0.47 h (n = 6). Although the number of sporogenic divisions differed for microspore and macrospore formation, development times for the two processes were similar: 3.0–6.3 and 4.0 h, respectively.

Host–parasite interactions and parasite generation time. Infested ciliates remained active and exhibited normal swimming and feeding patterns; however, the nuclear configuration of parasitized hosts was abnormal, and infested cells appeared unable to divide. The macronuclei of ciliates infested by immature parasites were typically displaced poleward and those of hosts harboring mature trophonts were irregular in profile and often formed dense aggregates (Figs. 4, 6, 7, 9). Of the several thousand parasitized *E. pectinis* examined during this study, only one host had progressed beyond the replication band stage of the nuclear cycle and none were undergoing cytokinesis.

To examine host–parasite interactions further, a natural population of *E. pectinis* infested by *D. cachoni* was isolated from

←

Fig. 18. A. Growth dependent relationships between morphological variables. Correlation coefficients are given for samples of "n" measurements. B. Data points located on the abscissa represent individuals with fragmented or resorbed nucleoli and were not included in the correlation analysis.

→

Figs. 19–30. Sporogenesis and spore morphology in *D. cachoni*. Bars = 20 μm unless otherwise noted. **19–23.** Events associated with microspore formation. The same specimen is shown soon after the host was ingested and at 0.8, 1.2, 1.5, and 4.3 h elapsed time; phase contrast microscopy. **19.** Post-phagotrophic stage with partially condensed food mass (f) inside a larger transparent vacuole (arrow). **20.** Second cytokinesis showing transverse fissions, food mass (f) located in the posterior sporocyte, and division of the transparent vacuole (arrows). **21.** Posterior sporocytes have completed the fourth fission, whereas cells positioned toward the anterior of the host lorica have entered the fifth cytokinesis and show a more oblique plane of division; food mass (f). **22.** Sixth/seventh sporogenic division. **23.** Very late stage in sporogenesis illustrating dense packing of sporocytes. **24–26.** Protargol impregnations of sporogenic stages. **24.** A sporocyte prior to the first cytoplasmic division. Two mitotic figures (arrows) and short v-shaped chromosomes are evident. **25.** Sporocytes during the second cytokinesis, each containing four nuclei. **26.** Late sporogenic divisions. **27.** Microspores dispersing from the host lorica; phase contrast. **28.** Protargol-impregnated microspores viewed with phase

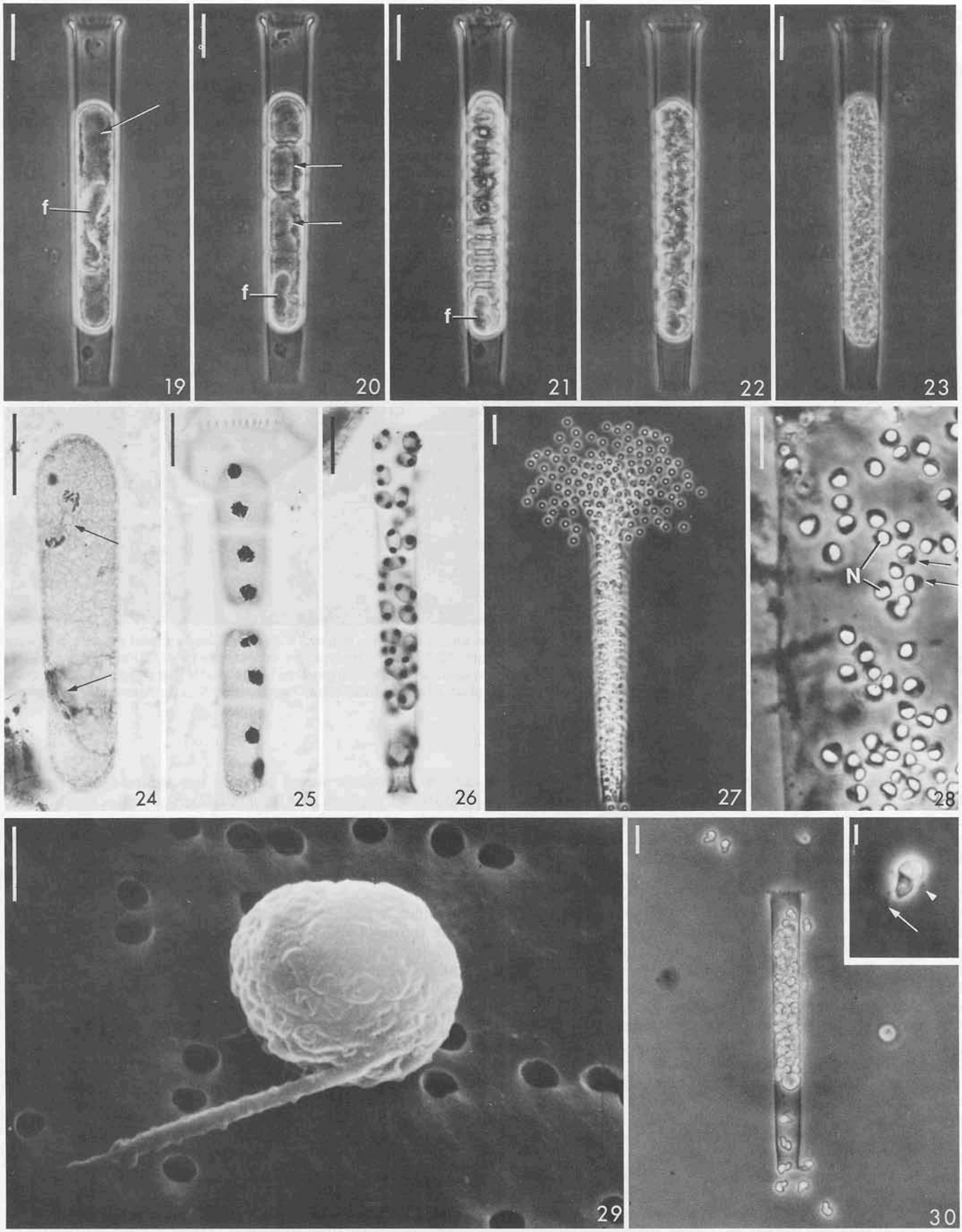

contrast optics. Bar = 5 μm. Spore nuclei (N) impregnate darkly with protargol, but appear white in phase images. An argentophilic granule is located at the base of each flagellum (arrows). **29**. SEM of a microspore showing the single short flagellum. Bar = 1 μm. **30**. Macrospores migrating from the host's lorica; phase contrast. Inset shows position of the transverse and posterior flagella (arrowhead and arrow, respectively) in living specimens. Bar = 5 μm.

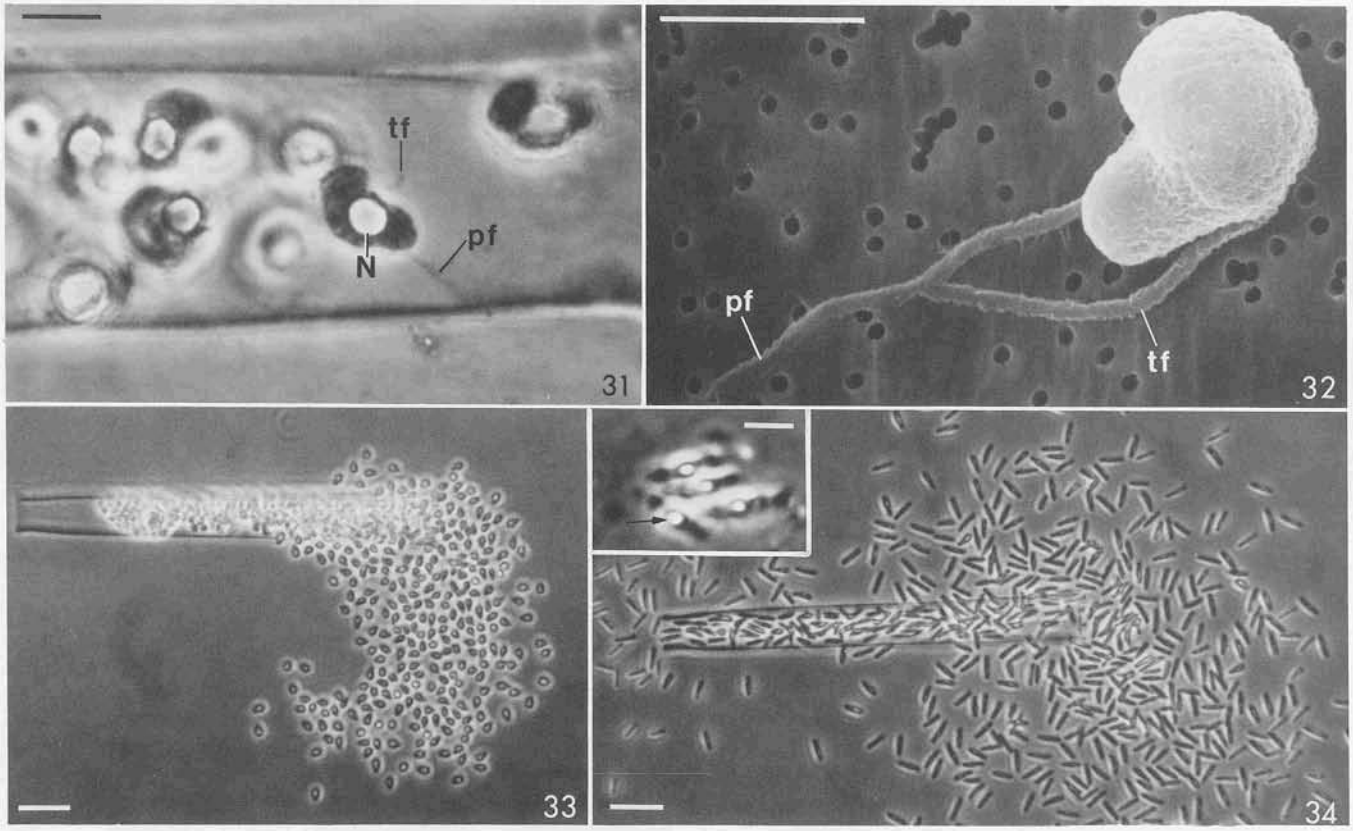

Figs. **31–34**. Macrospores and "cysts" of *D. cachoni*. Bars = 20 μm unless otherwise noted. **31**. Protargol-impregnated macrospores with nucleus (N), posterior flagellum (pf), transverse flagellum (tf). Bar = 5 μm. **32**. SEM of a macrospore showing posterior (pf) and transverse (tf) flagella. A shallow girdle formed at the indentation between the globular episome and smaller hyposome is also visible. Bar = 5 μm. **33**. Immature cyst-like spores; phase optics. **34**. Same spores as Fig. 33, but photographed 2 h later. Inset shows "cysts" after 5 days. Arrow indicates ovoid inclusion thought to be the cyst nucleus. Bar = 5 μm.

surface waters of the Chesapeake Bay (37°39′N lat.; 76°12′W long.) at 1200 h (T_0), 23 July 1986 and monitored for 48 h. Data on the abundance of hosts, trophonts, and sporogenic stages, and percent infested hosts are summarized in Fig. 35A, B. During the first 24 h (T_0–T_{24}), the host population increased steadily and reached a peak density (4.2 ml^{-1}) that was approximately 50% higher than initial cell concentrations (2.8 ml^{-1}). During this period, the percentage of infested hosts varied between 10.1 and 23.2% but showed no consistent directional trend. Host abundance was sharply lower at T_{30} and continued to decline thereafter. The initial drop in host numbers was accompanied by a two-fold increase in parasite prevalence with the percentage of infested hosts remaining high in later samples.

Trophont abundance increased soon after the start of the experiment, doubled by T_{30}, and then fell abruptly. The number of sporogenic stages was relatively unchanged between T_0 and T_{18} but increased in subsequent samples and reached a maximum following the peak in trophont density. This 18–24-h lag between observed increases in trophont and sporogenic stages coupled with the short interval between their highest densities suggests that the transition from trophont to sporogenesis is a relatively rapid process that takes <24 h. Through T_{30}, trophonts and sporogenic stages represented 79.5 ± 2.06% and 20.5 ± 2.06% (n = 7) of the parasite population, respectively; however, as trophont density decreased, sporogenic stages continued to increase and accounted for >40% of total parasites at T_{36} and T_{48}. The proportional relationship between % trophonts and % sporogenic stages, prior to the decline in the parasite population, suggests that trophont development is roughly four times longer than the duration of sporogenesis. This proportionality indicates that trophont maturation requires ~18 h, which closely corresponds to the lag-time noted above.

DISCUSSION

Cachon & Cachon (3) have recently reviewed criteria that define the dinoflagellate nature of parasitic genera. Classification of these organisms as dinoflagellates rests largely on the morphology of the spores and various aspects of mitosis. Previously described species of parasitic dinoflagellates produce spores that have a sulcus and girdle, although often poorly developed, and always possess a transverse and a trailing flagellum. Unlike free-living dinoflagellates, most parasitic forms do not have condensed chromosomes throughout their life cycle and the chromosomes of some parasites are never condensed. The mitotic apparatus of parasitic species, however, resembles that of other dinoflagellates as 1) the nuclear envelope remains intact and facilitates segregation of the chromosomes and 2) the extranuclear spindle is associated with a cytoplasmic channel(s) that traverses the nucleus. *Duboscquella cachoni* differs from all other parasitic dinoflagellates by forming microspores that have only a single flagellum and lack a bipartite structure.

Three genera of dinoflagellates—*Amoebophrya, Duboscquella,* and *Duboscquodinium*—contain species known to parasitize tintinnine hosts. *Amoebophrya* differs from the other two genera

by 1) the presence of flagella during trophont development and 2) the formation of a "mastigocoel" (i.e. a cavity produced by the invagination of the episome into the hyposome) prior to the phagotrophic phase (2, 3). Discrimination of the other genera is less certain as *Duboscquodinium* is a rather enigmatic taxon that contains two poorly described species. Grassé (published by Chatton [5]) characterized species of *Duboscquodinium* as having 1) a trophont with typical dinoflagellate nucleus and moniliform chromosomes, 2) a differential first sporogenic division that produces a sporocyte and a trophocyte, and 3) spores that resemble *Gymnodinium*. The parasite described here is placed in the genus *Duboscquella* as it exhibits several structural features common to species of *Duboscquella* and lacks morphological and developmental traits that characterize species of *Amoebophrya* and *Duboscquodinium*.

Identification of *Duboscquella* species centers largely on trophont morphology; however, attributes including host organism(s), sporogenic development, and spore morphology are also valuable in distinguishing members of this genus (Table II). Species fall into two groups represented by 1) *D. anisospora, D. caryophaga, D. enemata, D. melo,* and *D. nucleocola,* all of which have a shield that is highly sculptured by ribs and furrows, and 2) *D. tintinnicola, D. aspida,* and *D. cachoni,* which either lack grooves or have only a single prominent furrow. Among this second group, *D. cachoni* differs from *D. tintinnicola* and *D. aspida* by the size and shape of the trophont, the pattern of sporogenesis, and spore morphology. In addition, the trophont of *D. cachoni* differs from that of *D. aspida* by having a reduced sagittal furrow, a closed perinematic ring, and a shorter, more broadly funneled lamina pharyngea.

TABLE I. *Morphological data for life history stages of* D. cachoni *from type host and locality.*

Life history stage and attribute	Mean (±SE) (μm)	Range (μm)	Sample size
Trophont			
Somatic length	—[a]	3.4–47.1	50
Somatic width	—[a]	3.4–12.8	50
Nuclear length	—[a]	2.2–15.7	50
Nuclear width	—[a]	2.2–10.2	50
Nucleolar diameter	—[a]	1.4–4.5	50
Major axis of perinematic ring	—[a]	5.0–33.9	50
Maximum width of lamina pharyngea	1.9 (±0.08)	1.5–2.3	10
Post-phagocytosis			
Somatic length	70.8 (±2.66)	33.7–95.0	32
Somatic width	14.5 (±0.29)	12.1–20.2	32
Nuclear length	13.8 (±0.40)	10.8–15.5	11
Nuclear width	10.5 (±0.29)	8.8–11.6	11
Macrospore			
Somatic length	6.6 (±0.10)	5.4–7.9	30
Somatic width	4.4 (±0.05)	3.9–4.9	30
Nuclear length	2.9 (±0.05)	2.4–3.5	30
Nuclear width	2.5 (±0.04)	2.1–3.0	30
Microspore			
Somatic diameter	2.2 (±0.08)	1.6–3.1	30
Nuclear length	1.3 (±0.03)	1.0–1.6	30
Nuclear width	1.7 (±0.06)	1.3–2.6	30
"Cyst"			
Somatic length	6.0 (±0.20)	4.3–7.6	20
Somatic width	1.4 (±0.05)	1.0–1.8	20
"Nuclear" diameter	1.2 (±0.06)	0.7–1.6	20

[a] Data not given because measurements vary with developmental state of the trophont and yield mean values that depend on population age structure.

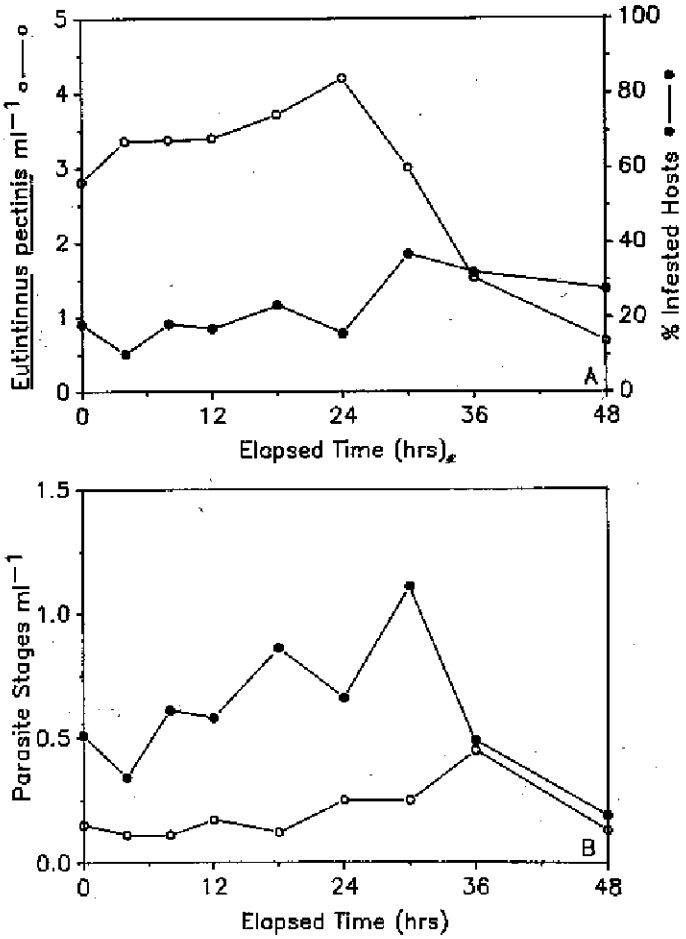

Fig. 35. Data for the study of a natural host–parasite assemblage. A. Abundance of *Eutintinnus pectinis* (○) and percentage of individuals infested by *Duboscquella cachoni* (●). B. Temporal occurrence of trophonts (●) and sporogenic stages (○) of *D. cachoni*.

Unlike other *Duboscquella* species, sporogenesis in *D. cachoni* results in a tightly packed cluster of sporocytes which remains within the host lorica. Three kinds of spores are produced and two of these are unique. Specifically, microspores of *D. cachoni* have only one flagellum and the non-motile spindle-shaped spore appears to be a resting life history stage. Cyst-like spores have been previously reported for *D. enemata*; however, these were not resting stages and more closely resembled the temporary pellicle cyst of other dinoflagellates (2). Macrospores of *D. cachoni* are similar in shape to those of other species, particularly *D. anisospora,* but differ in size and position of flagellar bases. In *D. cachoni,* basal bodies are located on the rounded surface opposite the indentation formed between the episome and hyposome, whereas the flagella of other species originate at this indentation (2). The number of spores produced infestation^{-1} has been documented for only one other species of *Duboscquella, D. aspida.* In that parasite, spore production is more than an order of magnitude greater than observed in *D. cachoni.*

Growth and development of *D. cachoni* appear to be much more rapid than in other *Duboscquella* species. Sporogenesis in *D. cachoni* only requires ~5 h, but lasts 2–3 days in *D. aspida*

TABLE II. *A summary of attributes that characterize* D. cachoni *and previously described species of* Duboscquella.

Species of *Duboscquella*	Host species	Trophont morphology/ development	Sporogenesis	Spore morphology	Refs.
D. tintinnicola	*Favella ehrenbergi* *Tintinnopsis campanula* *Codonella galea*	spherical to ovoid; maximum size ~100 μm; large vesicular nucleus with compact nucleolus	sporogenesis initiated inside the host; large sporocytes (~20 μm diam.) emerge from the host and continue to divide	7–8 μm long; episome pointed, hyposome rounded; one flagellum directed anteriad, a second is wrapped transversely around the body	4, 7, 10
D. anisospora	*Favella* sp.	similar to *D. tintinnicola* but with several furrows that nearly encircle the body; undefined size	not well described; similar to *D. tintinnicola*	microspores 12.5 μm, macrospores 20 μm long; spores similar in shape with a globular episome and a narrower pointed hyposome; two flagella, one trailing and one transverse with large mastigonemes	5
D. aspida	*Favella ehrenbergi* *Coxliella laciniosa* *Tintinnopsis campanula* *Eutintinnus franknóii*	ovoid, ≤80 μm diam. with flattened episome; elliptical shield is underlain by a fibrillar lattice; sagittal furrow conspicuous and bisects the shield; perinema forms an open circle with overlapping ends; lamina pharyngea well developed; nucleus spherical, ~40 μm diam.; nucleolus is large in young trophonts, but absent in parasites ≥30 μm diam.; a substantial amount of host cytoplasm is ingested during the phagotrophic phase	sporogenesis occurs outside the host; cytokinesis is perpendicular to a row of basal bodies positioned along the sagittal furrow; sporocytes remain connected and form long beaded strands; food vacuole does not divide	microspores (~50,000) measure 2 × 3 μm and have two short (~1 μm) flagella; macrospores (~1000) are 6–7 μm long and have a trailing and transverse flagellum each ~12 μm in length; microspores comma-shaped with bulbous episome; macrospores bean-shaped	2
D. cnemata	*Favella ehrenbergi*	ovoid, ≤60 μm; 20–30 fibers radiate from the perinema and follow furrows that spiral toward the center of the convex shield; lamina pharyngea forms a short funnel; phagotrophic stage not observed	occurs outside of host; sporocytes not aggregated	one type of spore described, 3–4 μm long, similar in shape to macrospores of *D. aspida*	2
D. caryophaga	*Strombidium* sp. *Strombilidium* sp. *Prorodon* sp.	mature trophont is spherical, ~30 μm diam.; during growth, the parasite digests host's nucleus; the shield resembles that of *D. cnemata* but only has ~10 grooves; lamina pharyngea reduced to a twisted filament; nucleolus absent in trophonts >15 μm	unknown; presumed to occur outside the host	unknown	2
D. melo	*Noctiluca miliaris*	young trophonts are bean-shaped but become spherical during growth, mature trophonts 50–80 μm diam. and have ~30 meridional furrows; several flagella are positioned along one of these furrows; no phagotrophic stage	sporogenesis takes place inside the host pellicle; all divisions are perpendicular to meridional furrows; flagellated sporocytes remain linked in chains	macrospores 8–10 μm, microspores 4–5 μm in length; transverse and trailing flagella are ~12 μm long; spores are bean-shaped with hyposome slightly larger than episome	2
D. nucleocola	*Leptodiscus medusoides*	early stages are located inside the host nucleus, are spherical (~20 μm diam.) and have an annular constriction; mature trophonts ≤125 μm diam.; a convex shield is present in parasites >70 μm diam.; ~100 furrows rib the shield; digestive vacuole not formed	sporogenesis proceeds outside the host with flagellated sporocytes forming motile chains	unknown	2

TABLE II. *Continued.*

Species of *Duboscquella*	Host species	Trophont morphology /development	Sporogenesis	Spore morphology	Refs.
D. cachoni	*Eutintinnus pectinis*	trophonts spherical at first and become ovoid with growth; mature trophonts very elongate, ≤50 μm × ~10 μm; convex shield present late in development; perinema forms a closed ellipse with short delicate fibrils radiating beneath the shield; shallow sagittal furrow transects ~¼ the shield; lamina pharyngea short, broadly funnelled; nucleus ovoid; large nucleolus absent in mature trophonts; entire host cell ingested during phagotrophic phase	sporogenesis outside the host; first few cytoplasmic divisions are transverse with later cleavages oblique to longitudinal; sporocytes remain clustered until spores are fully differentiated; food mass passes to most posterior daughter cell	microspores (~500) are spherical (~2 μm diam.) with a single short flagellum (~5 μm); macrospores (~50) are 4 × 7 μm, have a globular episome, a smaller rounded hyposome and have a long (~15 μm) posterior and short (~10 μm) transverse flagellum; cyst-like spores (~600) are spindle-shaped and measure 4 × 6 μm	

and ~24 h in *D. melo* (2). Similarly, trophont maturation in *D. cachoni* occurs in <1 day, but requires 3–4 days in *D. aspida*. Dissimilar development times for these parasites may reflect species differences but are probably exaggerated as data for *D. cachoni* are from populations at 23–27°C while observations for *D. aspida* and *D. melo* were made at ~20°C.

Phagotrophy in *D. cachoni* follows a morphogenetic process very similar to that of *D. aspida* (2), yet the final result is somewhat different. *Duboscquella cachoni* generally ingests the entire host while *D. aspida* only consumes a portion of the host's cytoplasm. Thus, unlike *D. aspida*, infestations of *D. cachoni* are invariably fatal to the host. Furthermore, the abnormal nuclear condition and absence of division stages among parasitized *E. pectinis* suggest that *D. cachoni* disrupts the host's cell cycle and prevents reproduction.

Cachon (2) reported an incidence of *D. aspida* infestation in *Favella* populations approaching 100% and argued that death due to parasitism may cause abrupt declines in host abundance. Recently, Stoecker et al. (14) noted a moderately high incidence of *Duboscquella* infestation in *Favella* sp. and suggested that parasitism may have been partly responsible for differences in net growth rate of this ciliate in field samples and laboratory cultures. Results of the field study conducted here show a dramatic increase in parasite prevalence coupled with the decline in host abundance and suggest that, under appropriate conditions, *D. cachoni* may have a significant impact on its host's population. The downward shift in host density occurred well after the start of the experiment and raises the possibility that confinement effects may have contributed to the death of host cells. Such effects, however, were not apparent in previous 36-h studies of non-parasitized ciliate populations (6).

Highly virulent parasites, especially those that reduce or prevent reproduction of infected organisms, are likely to regulate host populations (1). Consequently, *D. cachoni* and other parasitic dinoflagellates may strongly influence the population dynamics of host species. Epizootic infestations may cause mass mortality of tintinnine ciliates and produce fine- to coarse-scale patchiness in host populations. Parasitic dinoflagellates that kill tintinnine ciliates consume a potential food source of copepods and other larger zooplankton and during periods of high parasite prevalence may have a greater influence on ciliate populations than metazoan predators. Unlike conventional predator–prey interactions that transfer energy to higher trophic levels, parasitism typically passes matter from larger to smaller organisms. If dinoflagellate infestations are common in ciliate populations, then parasitism among protists may represent an important trophic relationship that cycles biomass within marine microbial food webs.

LITERATURE CITED

1. Anderson, R. M. & May, R. M. 1981. The population dynamics of microparasites and their invertebrate hosts. *Philos. Trans. R. Soc. Lond. B, Biol. Sci.*, **291**: 451–524.

2. Cachon, J. 1964. Contribution a l'étude des péridiniens parasites. Cytologie, cycles évolutifs. *Ann. Sci. Nat. Zool.*, **6**: 1–158.

3. Cachon, J. & Cachon, M. 1987. Parasitic dinoflagellates, *in* Taylor, F. J. R., ed., *The Biology of Dinoflagellates.* Blackwell Sci. Pub., Oxford, pp. 571–610.

4. Chatton, E. 1920. Les peridiniens parasites. Morphologie, reproduction, ethologie. *Arch. Zool. Exp. Gen.*, **59**: 1–475.

5. Chatton, E. 1952. Classe des Dinoflagellés ou Péridiniens, *in* Grassé, P.-P., ed., *Traité de Zoologie,* Masson et Cie, Paris, **1**: 309–390.

6. Coats, D. W. & Heinbokel, J. F. 1982. A study of reproduction and other life cycle phenomena in planktonic protists using an acridine orange fluorescence technique. *Mar. Biol.*, **67**: 71–79.

7. Duboscq, O. & Collin, B. 1910. Sur la reproduction sexuée d'un protiste parasite des tintinnides. *C. R. Acad. Sci., Paris,* **151**: 340–341.

8. Entz, G. 1909. Studien uber Organisation und Biologie der Tintinniden. *Arch. Protistenkd.*, **15**: 93–226.

9. Galigher, A. E. & Kozloff, E. N. 1971. *Essentials of Practical Microtechnique,* 2nd ed. Lee and Febiger, Philadelphia.

10. Hofker, J. 1931. Studien über Tintinnoidea. *Arch. Protistenkd.*, **75**: 315–402.

11. Lee, J. J., Small, E. B., Lynn, D. H. & Bovee, E. C. 1985. Some techniques for collecting, cultivating and observing protozoa, *in* Lee, J. J., Hutner, S. H. & Bovee, E. C., eds., *Illustrated Guide to the Protozoa.* Allen Press, Lawrence, Kansas, pp. 1–7.

12. Lohmann, H. von. 1908. Untersuchungen zur Feststellung des vollstandigen Gehaltes des Meeres an Plankton. *Wiss. Meeresunters.*, **10**: 296–297.

13. Parducz, B. 1967. Ciliary movement and coordination in ciliates. *Int. Rev. Cytol.*, **21**: 91–128.

14. Stoecker, D. K., Davis, L. H. & Provan, A. 1983. Growth of *Favella* sp. (Ciliata: Tintinnina) and other microzooplankters in cages incubated *in situ* and comparison to growth *in vitro*. *Mar. Biol.*, **75**: 293–302.

15. Utermöhl, H. 1931. Neue Wege in der quantitive Erfassung des Planktons. *Verh. Int. Ver. Theor. Angew. Limnol.*, **5**: 567–596.

Received 21 III 1988; accepted 26 VI 1988